Volume 49
Number 30
14 August 2025
Pages 12887–13210

NJC

New Journal of Chemistry

A journal for new directions in chemistry

rsc.li/njc

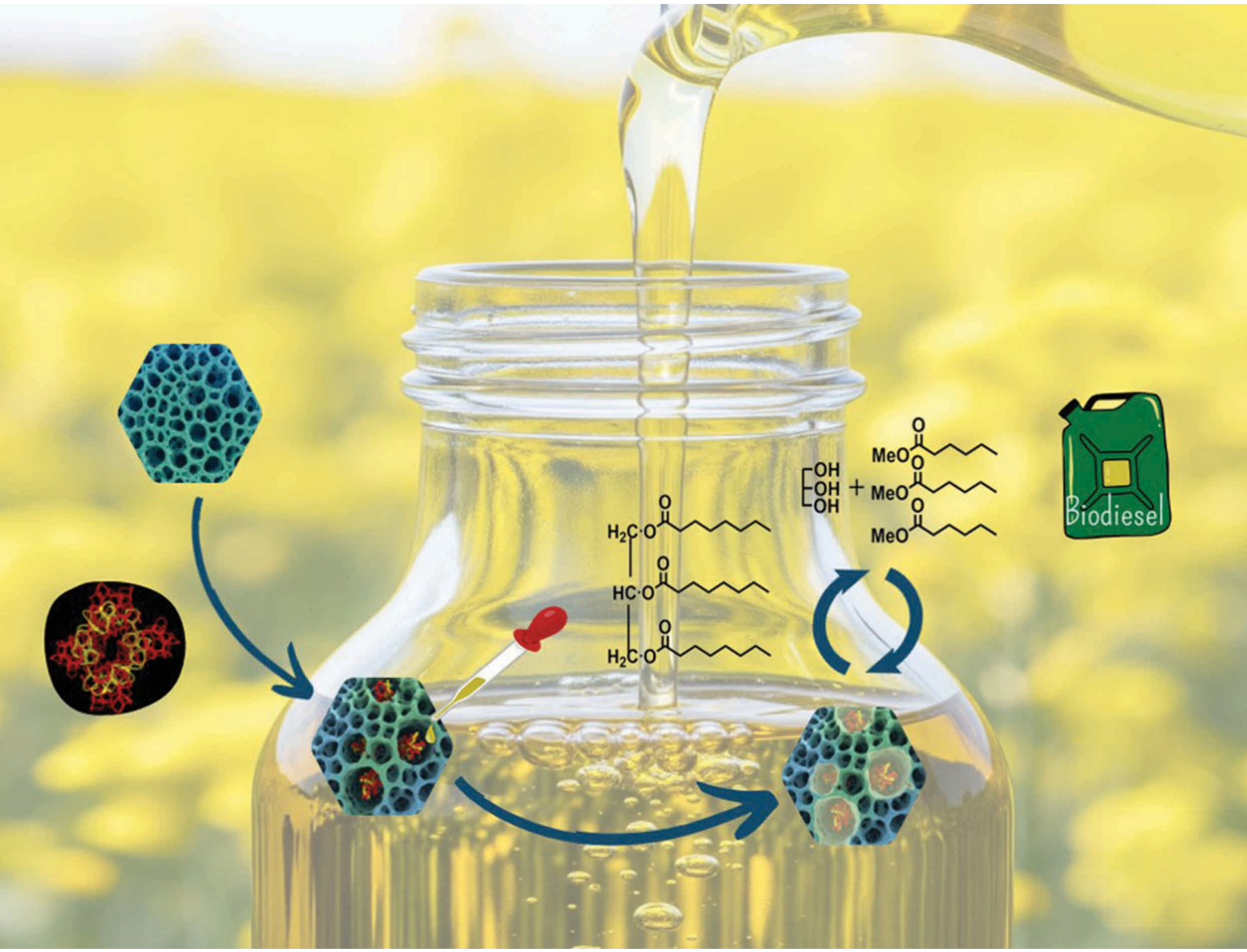

ISSN 1144-0546

ROYAL SOCIETY OF CHEMISTRY

PAPER

Christine Gérardin-Charbonnier, Jean-Luc Blin *et al.*
Supramolecular biosourced hydrogelator: a green tool for tailoring the pore size of mesostructured silica for enzyme immobilization

cnrs

NJC

PAPER

View Article Online
View Journal | View Issue

Cite this: *New J. Chem.*, 2025, **49**, 12931

Supramolecular biosourced hydrogelator: a green tool for tailoring the pore size of mesostructured silica for enzyme immobilization†

Christine Gérardin-Charbonnier,*[a] Karine Assaker,[b] Mélanie Emo,[b] François Vibert[b] and Jean-Luc Blin *[b]

Received 23rd September 2024,
Accepted 28th April 2025

DOI: 10.1039/d4nj04160g

rsc.li/njc

Herein, we reported the design of a supported biocatalyst through the physisorption of *Mucor miehei* lipase (Mm-L) onto SBA-15, followed by the addition of a supramolecular biosourced hydrogelator to reduce the mesopore diameter and prevent enzyme leaching. Prior to enzyme immobilization, the effect of the hydrogel on the structural and textural characteristics of the mesostructure was investigated. Results showed that the presence of the hydrogel did not affect mesopore ordering but successfully reduced the mesopore diameter as targeted. Subsequently, as a potential application of mesopore size control by the hydrogel, the supported biocatalyst was prepared and tested for the synthesis of biodiesel through the transesterification of rapeseed oil with methanol. The reaction was performed under previously optimized conditions. Reusability tests of the supported biocatalysts showed that, in the presence of the hydrogel, the biocatalyst exhibited higher operational stability, remaining effective for up to 5 consecutive runs, than the corresponding physisorbed enzyme without the hydrogel, which was efficient for only 2 consecutive runs. This clearly demonstrated that the addition of the hydrogel limited enzyme leaching.

1. Introduction

Owing to their features such as high specific surface area and pore volume, mesostructured silicas have applications in various domains, including adsorbents, catalysts, host matrixes for electronic and photonic devices, drug delivery and sensors.[1–5] In particular, they can be used as matrices for enzyme immobilization.[6–11] The presence of silanol groups facilitates enzyme immobilization, and surface modification of the material through grafting functional groups *via* silylation allows modulation of the surface physicochemical characteristics.[12] There are various methods to encapsulate the enzyme, such as physical adsorption, physical entrapment, cross-linking or covalent attachment (*i.e.* chemical adsorption).[9,13–15] However, physical immobilization is the most commonly used method for enzyme-based processes due to its simplicity, rapidity and low cost, as it does not require functionalized materials or toxic solvents. However, since this process relies on weak bonds, such as hydrogen bonds or van der Waals forces, its reuse capability is moderate due to the possible leaching of the enzyme. The main challenge is to reduce this phenomenon. Among the different mesostructured silicas, Santa Barbara Amorphous 15 (SBA-15) supports are widely used for enzyme immobilization due to their good stability under operational conditions, hydrophilic nature, high surface area (300–1500 $m^2\ g^{-1}$), regular and easily controllable pore diameters (2–40 nm), which are compatible with enzyme sizes, and high pore volume (around 1 mL g^{-1}).[15–17] Indeed, one of the most important parameters in enzyme immobilization is the pore size of the support.[18–20] It is well known that the closer the pore size of the support is to the diameter of the enzyme, the better the immobilization performance, as it provides better conformational stability and reduces the likelihood of structural modification of the adsorbed enzyme in the pores while preventing enzyme leaching.[18–20] Various strategies have been developed to control and tailor mesopore diameters. Post-synthesis treatments, surfactants of different chain lengths and variations in synthesis conditions (*e.g.*, pH and surfactant/silica ratio) can be employed to achieve this goal. Another way to tailor the pore diameter of mesostructured silica is by incorporating swelling agents during the synthesis.[21–27] Recently, much effort has been devoted to develop new ecodesigns[28,29] and to simplify the synthesis procedures[4,30] for

[a] *Université de Lorraine, Laboratoire d'Etudes et de Recherche sur le Matériau Bois, LERMaB, UR 4370, USC INRAE F-54506 Vandoeuvre-lès-Nancy cedex, France. E-mail: christine.gerardin@univ-lorraine.fr; Tel: +33 372745234*

[b] *Université de Lorraine, Laboratoire Lorrain de Chimie Moléculaire UMR CNRS 7053 L2CM, 54500 Vandoeuvre-lès-Nancy, France. E-mail: Jean-Luc.Blin@univ-lorraine.fr; Tel: +33 372745270*

† Electronic supplementary information (ESI) available. See DOI: https://doi.org/10.1039/d4nj04160g.

the mesostructured silica. Many research studies are focused on the templates and on the silica precursors, but few studies seem to concern the replacement of the organic additive used to tailor the size of mesopores. In this perspective, supramolecular biosourced hydrogelators appear to be excellent candidates as mesopore control agents, with a particular aim to reduce the mesopore diameter.

Interest in supramolecular or physical gels obtained from low-molecular-weight molecules has increased significantly over the last ten years.[31–33] Currently, this research is at the interface between chemistry, biology and nanotechnology.[34] The interest in these materials is, at the same time, theoretical, in terms of the comprehension of the fundamental mechanisms that control the phenomenon of aggregation, but also applicative in terms of the engineering of new molecular devices. Generally, these materials are sensitive to external stimuli, such as light or chemical species, which makes them interesting for use in sensors. They can also be used as footprints for inorganic structures, and have consequently found applications in catalysis or in the field of separation.[35] Other applications include the biomedical and cosmetic fields.[36] Gels obtained from low-molecular-weight compounds have a particular importance considering their biocompatibility and their biodegradability. They have also been used for wood preservation.[37,38] In this latter case, by mixing a hydrophilic biocide with a thermoreversible hydrogel, a supramolecular network is formed, which traps the biocide within the wood as the solution gels when the temperature drops, which then prevents the biocide from leaching out when the wood is used in outdoor conditions. Hydrogels have also been used as a template in the synthesis of mesoporous materials.[39]

In a previous work, we shown that SBA-15 is a suitable support for the physisorption of *Mucor miehei* lipase (Mm-L),[40] and that the obtained supported biocatalysts could effectively be used to catalyze the transesterification of rapeseed oil with methanol, giving up to a 76% yield. The reaction parameters (methanol/oil molar ratio, catalyst weight, temperature, water) were optimized using an experimental design methodology,[41] and the results indicated that methanol/oil molar ratio (M/O), % wt water, and the interaction between the M/O ratio and water were the key factors affecting the methyl ester yield in the Mm-L-catalyzed transesterification of rapeseed oil. The optimal conditions for the transesterification were found to be: reaction temperature of 24 °C, alcohol/oil molar ratio of 1 : 1, and water content of 2.5% w/w. Under these reaction conditions, the methanol was totally consumed and around one-third of the triglycerides was converted. However, after the first run, the leaching of the lipase occurred and the supported biocatalyst could not be reused. This was attributed to the weak interaction modes (hydrogen, hydrophobic, electrostatic and van der Waals interactions) between the support and the enzyme. As explained above, a means to overcome this scientific bottleneck is by modification of the surface property by grafting alkylsilanes on the hydroxyl groups of the support surface or by covalent immobilization.[9] However, these strategies imply a chemical modification of the support's surface, which can also modify the enzyme activity. Here, as a potential application of the mesopore control strategy by the addition of a hydrogel, we propose introducing a supramolecular biosourced hydrogelator after the physisorption of Mm-L to limit the enzyme leaching by reducing the mesopore size. Specifically, we propose utilizing a simple supramolecular gelling system, namely a glycerol carbamate derivative. This method is eco-friendlier and has the benefit that no surface modification of the mesostructured matrix is required. Thus, as a first part of our work, we investigated the effect of the addition of a supramolecular biosourced hydrogelator on the mesopore diameter of SBA-15.

2. Experimental

2.1. Materials

Pluronic P123 and the *Mucor miehei* lipase (Mm-L) were provided by Sigma Aldrich. The products were used as received, without any further purification. The quantity of proteins contained in the commercial powder, determined by the Bradford assay, was around 2.2%. Methyl dodecanoate (99%), used as internal standard for GC-FID analysis, was supplied by Alfa Aesar. Deionized water was obtained using a Milli-Q water purification system. Acetonitrile was obtained from Sigma Aldrich. All the reactants for the preparation of the gelator were purchased from Acros Organics (Noisy le Grand, France), or Sigma Aldrich Chimie SARL (St Quentin Fallavier, France), or Alfa Aesar (Johnson Matthey Company, Schiltigheim, France).

2.1.1. Preparation of the hydrogel. To obtain the hydrogel containing 5 wt% of carbamate, 150 mg of 2,3-dihydroxypropyl tetradecylcarbamate was added to 2.850 g water and the mixture was sonicated for 2 h at 80 °C. The mixture was then cooled under vigorous stirring until the white hydrogel was obtained. A similar procedure was adopted with 205 mg of 2,3-dihydroxypropyl tetradecylcarbamate and 1.845 g of water to prepare the hydrogel with 10 wt% of carbamate (Scheme 1).

2.1.2. Preparation of SBA-15. SBA-15 silicas were synthesized by a sol–gel process according to a standard procedure in the presence of structure-directing agents.[40] In a typical synthesis, 2.66 g of P123 were dissolved in 100 mL of a hydrochloric acid solution (1 M). Then, 4.17 g of TMOS, the inorganic precursor, were added, and the mixture was stirred at room temperature for 30 min. Afterwards, the solution was transferred into an autoclave and heated at 40 °C for 24 h, followed by heating at 100 °C for 48 h. The mesoporous silica material was obtained after surfactant extraction by ethanol over 48 h using a Soxhlet apparatus. The obtained powder was then dried under vacuum overnight to afford SBA-15 as a white powder.

2.1.3. Physisorption of the lipase. The enzyme was dissolved in 4 mL of a solution of Tris buffer solution (0.2 M) at pH 6. According to other studies led previously by our group,[40,41]

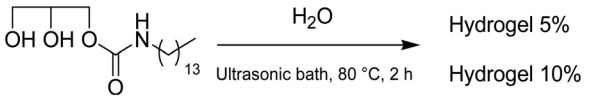

Scheme 1 The hydrogel preparation.

the concentration of enzyme was fixed at 10 mg per mL of solution. Then, 20 mg of SBA-15 material was added to the solution and this was then left under gentle agitation at room temperature for 4 h to reach equilibrium. Finally, the solution was filtered and the recovered solid was washed 3 times with 5 mL of the buffer solution, before being left to dry at room temperature for at least 12 h.

2.1.4. Incorporation of the hydrogel in the support. A specific amount of the hydrogel (×mg) containing either 5 or 10 wt% of carbamate was heated at 40 °C under stirring for 10 min. Then, 100 mg of SBA-15 was added and the mixture was stirred for 1.5 h at 40 °C, then filtrated and washed 3 times with 0.1 mL of deionized water. The recovered solid was left to dry at room temperature for at least 12 h. The value of x was fixed to vary the hydrogel/SBA-15 weight ratio from 0 to 7. After the adsorption of the lipase, a similar methodology was applied with 140 mg of hydrogel and 20 mg of the biocatalyst, *i.e.* SBA-15 with the physisorbed lipase.

2.1.5. Transesterification reaction. Details on the optimization of the transesterification conditions are provided in our previous papers.[40,41] Here, samples were prepared by mixing 600 μg of rapeseed oil with 26 μL of anhydrous methanol to obtain a molar ratio of alcohol to oil equal to 1 in order to avoid denaturation of the lipase due to methanol toxicity. The average molecular weight of the oil was taken to be equal to 881.6 g mol^{-1}, according to the value determined by Hajar *et al.*[42] Next, 14 μL of water was added to the solution. Finally, 10 mg of the mesoporous material containing the physisorbed lipase was added to the mixture.

The reaction was done at room temperature under agitation (100 rpm) for 72 h. Before the GC-FID analysis, the samples were centrifuged for 15 min to separate the mesoporous material from the products of the reaction. The products were analyzed after this time. Note, under the framework of this article, no kinetic study was performed. The transesterification reaction was investigated in detail and reported in our previous paper.[41]

2.1.6. Reuse of the biocatalyst. For the reuse of the biocatalyst, the initial amount of SBA-15 material was fixed at 150 mg for the physisorption. The corresponding amounts of rapeseed oil, anhydrous methanol and water were calculated for the first use and were equal to 6 mL, 0.26 mL and 0.14 mL, respectively. After each use, the mesoporous material was washed 2 times with 5 mL of hexane. Based on the amount of material recovered after washing, the corresponding quantities of reagents needed for the reaction were calculated and then added to the mixture.

2.1.7. Characterization of the mesoporous materials. Small angle X-ray scattering (SAXS) data were collected on a "SAXSess mc^2" instrument (Anton Paar), using a line of collimation system. This instrument was attached to an ID 3003 laboratory X-ray generator (General Electric) equipped with a sealed X-ray tube (PANalytical, $\lambda_{Cu,K\alpha}$ = 0.1542 nm) operating at 40 kV and 50 mA. Each sample was put between two sheets of Kapton®, inside an evacuated sample chamber, and exposed to an X-ray beam. Scattering of the X-ray beam was recorded by a CCD detector (Princeton Instruments, 2084 × 2084 pixels array with a 24 × 24 μm^2 pixel size) at 309 mm from the sample. Using SAXSQuant software (Anton Paar), the 2D image was integrated into one-dimensional scattering intensities $I(q)$ as a function of the magnitude of the scattering vector $q = (4\pi/\lambda)\sin(\theta)$, where 2θ is the total scattering angle. All the data were then corrected for background scattering from the cell and for slit-smearing effects by a desmearing procedure in SAXSQuant software, using the Lake method.

Nitrogen adsorption and desorption isotherms were determined on a Micromeritics TRISTAR 3000 sorptometer at −196 °C over a wide relative pressure range from 0.01 to 0.995. The specific surface area was calculated by the Brunauer–Emmett–Teller (BET) method (molecular cross-sectional area of N_2 = 0.162 nm^2). The pore diameter and the pore-size distribution were determined by the Barret–Joyner–Halenda (BJH) method[43] applied to the adsorption branch of the isotherm.

The infrared spectra were recorded on a Nicolet 8700 FTIR spectrometer, equipped with a KBr beam splitter and DTGS detector. The spectra in the diffuse reflectance mode were collected using Harrick Praying Mantis™ equipment. To perform the analysis, the mesoporous silica powder (5 wt%) was mixed with KBr. The reflectances R_s of the sample and R_r of the pure KBr, used as a non-absorbing reference powder, were measured under the same conditions. The relative reflectance is defined as $R = R_s/R_r$. The spectra are shown in pseudo-absorbance ($-\log R$) mode.

2.1.8. Quantification of the methyl esters-GC-FID analysis. Before the GC-FID analysis, the methyl esters were separated from the residual fatty acids by solid-phase extraction (SPE), using SPE C18-*S*-500/6 cartridges, supplied by Interchim. First, the cartridges were conditioned with 1 mL of acetonitrile. Then, 100 μL of the reaction products and 100 μL of a solution containing methyl dodecanoate as the internal standard (diluted in acetonitrile (1 : 10 (v/v))) were transferred into the cartridge. Acetonitrile was passed through the extraction device, until reaching a total volume of 10 mL. Finally, the obtained methyl esters solutions were diluted 10 times.

GC-FID was used to identify and quantify the methyl esters in the samples. The equipment consisted of a Shimadzu GC-2010 Plus instrument equipped with a flame ionization detector (FID). The capillary column mounted on the system was OV1 from OV Company (30 m × 0.25 mm ID × 0.25 μm). The conditions for the analyses were optimized and set as follows: the injection port of the GC was set at 280 °C and the samples were injected in the split mode with a split ratio of 3.0. The detector temperature was fixed at 280 °C. Nitrogen (99.999%) was used as carrier gas at a total flow rate of 12.6 mL min^{-1}. The column oven temperature was initially set at 145 °C for 3 min, then ramped at 3 °C min^{-1} to 155 °C and held there for 25 min, and finally ramped at a rate of 5 °C min^{-1} to 250 °C, where it was held for 5 min.

3. Results and discussion

3.1. Effect of the gel addition on the mesostructured silica in the absence of enzyme

In the absence of the hydrogel, the SAXS pattern of the bare SBA-15 exhibited four peaks at 11.0, 6.3, 5.4 and 4.1 nm (Fig. 1),

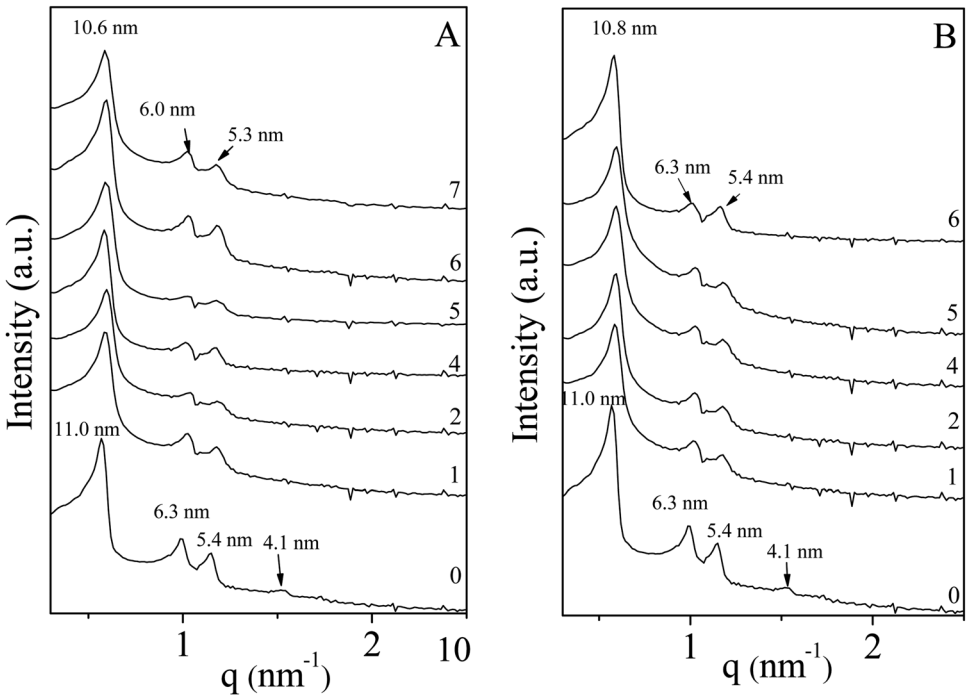

Fig. 1 Evolution of the SAXS pattern as a function of the hydrogel/SBA weight ratio. The hydrogel contains 5 wt% (A) or 10 wt% of tetradecylcarbamate (B).

characteristic of the (100), (110), (200) and (210) reflections of the hexagonal mesopore arrangement. Upon the addition of the hydrogel, regardless of the hydrogel/SBA-15 weight ratio, no significant modification of the SAXS pattern was noted (Fig. 1A and B). The hexagonal mesopore arrangement was maintained and no collapse of the mesostructure was detected. However, we could observe a slight decrease in the intensity of the secondary reflections, which may have been due to a partial filling of the mesopores by the hydrogel.

The bare SBA-15 exhibited a mixed type I/type IV isotherm according to the IUPAC classification[44] (Fig. 2), indicating the presence of both micropores and mesopores, as expected for such an ordered mesoporous silica.[45] An H1 type of hysteresis loop, with steep adsorption and desorption branches, was observed, which was in agreement with the presence of cylindrical mesopores. The specific surface area (S_{BET}) and total pore volume (V_p) values were 731 $m^2\ g^{-1}$ and 1.08 $cm^3\ g^{-1}$, respectively (Fig. 3). The mesopore diameter distribution determined using the BJH method was quite narrow and was centred at *ca.* 10.2 nm (see inset of Fig. 2).

After the introduction of the hydrogel, except for a decrease in the volume of nitrogen adsorbed, no significant change was noted in the shape of the adsorption branch of the isotherm (Fig. 2). The textural characteristics of SBA-15 were thus well maintained. However, the relative pressure at which capillary condensation took place was slightly shifted toward lower values. Since the p/p_0 position of the inflection point is related to the pore diameter, it could be inferred that a decrease in the mean pore diameter occurred when the preparation of the mesostructured silica was carried out in the presence of the hydrogel. This decrease in pore diameter was further confirmed by the pore-size distribution (see inset Fig. 2), with the maximum size shifted from 10.2 to 8.0 nm when the hydrogel/SBA-15 weight ratio changed from 0 to 6 for the hydrogel containing 5 wt% of tetradecylcarbamate (see inset Fig. 2A) and from 10.2 to 7.3 when the hydrogel/SBA-15 weight ratio was varied from 0 to 7 for the hydrogel containing 10 wt% of tetradecylcarbamate (see inset Fig. 2B). Since the d_{100} values observed by SAXS were not modified after the addition of the hydrogel, the variation of the mesopore diameter indicates the partial filling of the mesopores with the gel. This conclusion was further supported by the evolution of the specific surface area and of the pore volume in relation to the hydrogel/SBA weight ratio (Fig. 3).

Concerning the specific surface area, it decreased between 7% and 71% after the addition of the gel containing 5 wt% of carbamate and from 25% to 67% when the gel contained 10 wt% of carbamate. A similar trend was observed for the pore volume. For example, for the gel containing 5 wt% of carbamate, its values varied from 0.81 to 0.37 cm^3 g-STP^{-1}; *i.e.* a drop of 25% to 66%, when the hydrogel/SBA-15 weight was increased from 1 to 6 (Fig. 3).

From the SAXS and the nitrogen adsorption–desorption analyses, it could be inferred that the presence of the hydrogel did not affect the mesopore ordering and that it partially filled the mesopores.

The effective presence of the hydrogel was verified by infrared analysis. Below 1800 cm^{-1}, the spectra were dominated by a broad and intense band around 1150 cm^{-1}, with a maximum at 1084 cm^{-1} and a shoulder at 1214 cm^{-1}, characteristic of the antisymmetric stretching vibrational mode of the Si–O–Si siloxane bridges. The less intense absorption at 954 cm^{-1} was assigned to the Si–O stretching of free silanols. The disappearance of the silanols signals was noteworthy, in particular the sharp band at

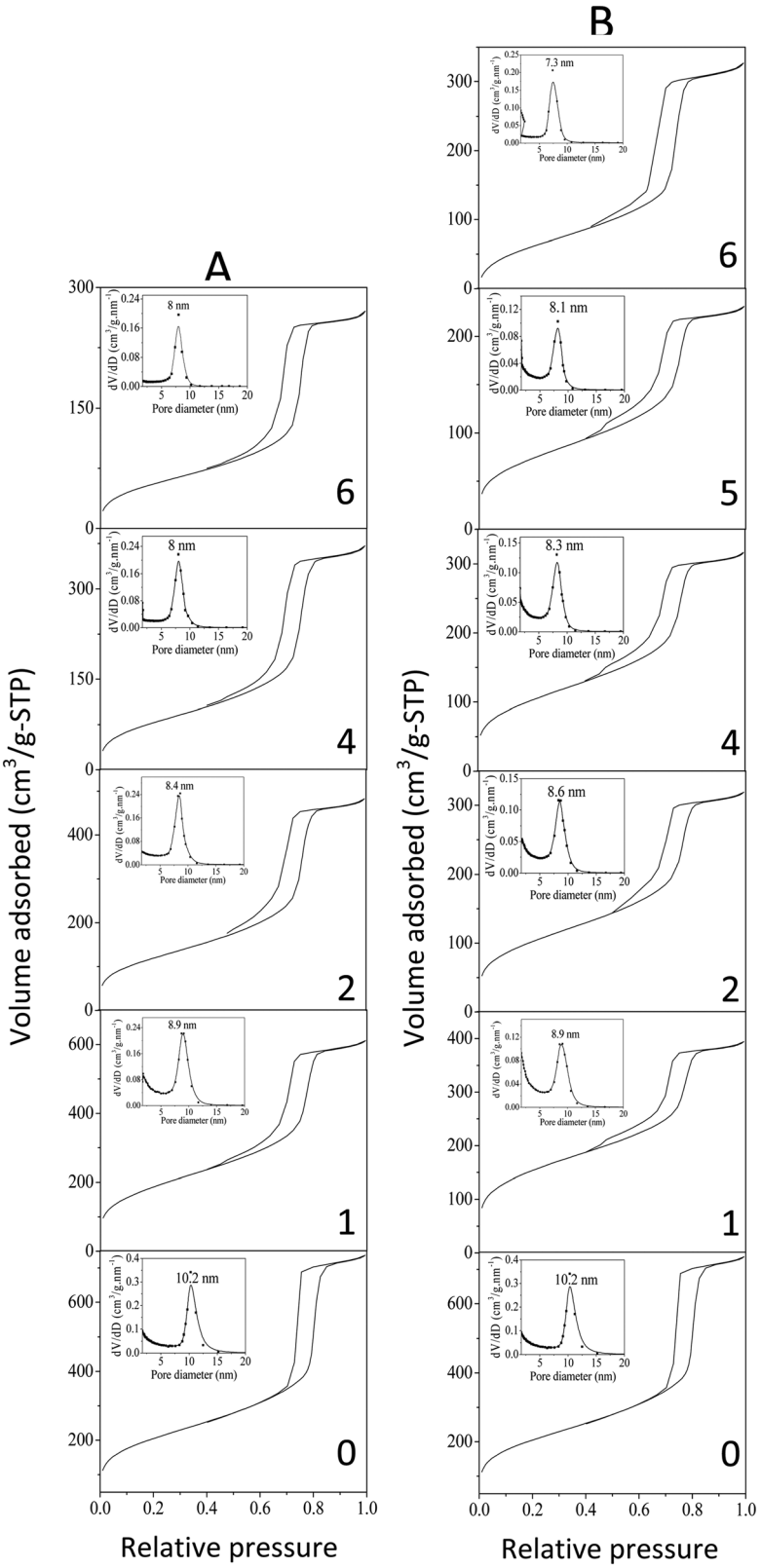

Fig. 2 Nitrogen adsorption–desorption isotherms with the corresponding mesopore size distribution (inset) as a function of the hydrogel/SBA weight ratio. The hydrogel contains 5 wt% (A) or 10 wt% of tetradecylcarbamate (B).

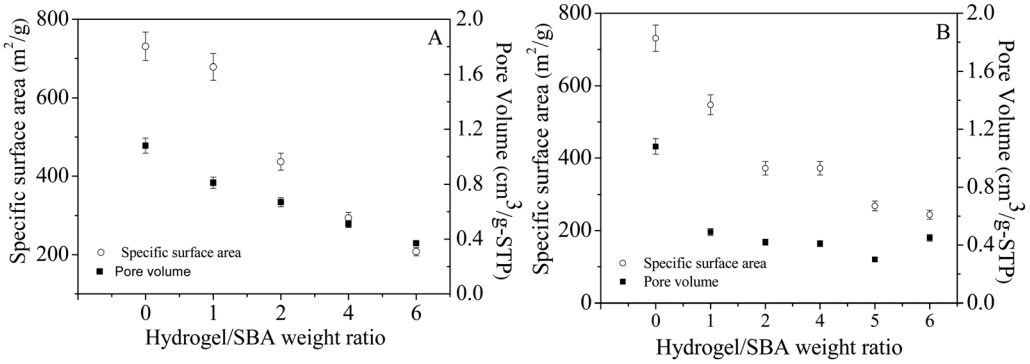

Fig. 3 Variation of the specific surface area and pore volume as a function of the hydrogel/SBA weight ratio. The hydrogel contains 5 wt% (A) or 10 wt% of tetradecylcarbamate (B).

3740 cm^{-1}, which is characteristic of the free silanols, due to the introduction of the gel into the mesopores (Fig. 4). The bands in the range of 2800–3000 cm^{-1} were assigned to the stretching modes of the alkyl chains of the gel and P123. Indeed, theses vibrations were also detected in the spectrum of the bare SBA-15, suggesting that a small amount of P123 was not removed during the template extraction step performed prior to the introduction of the hydrogel to free the mesopores. Nevertheless, their intensity increased with the increasing hydrogel/SBA weight ratio. This further confirms the presence of the hydrogel within the mesopores. The latter was unambiguously proven by the appearance of the C═O stretching vibrations and the N–H bending modes of the gel, which were located at around 1694 and 1538 cm^{-1}, respectively. These vibrations were not observed in the spectrum of the pure SBA-15, but started to appear as soon as the hydrogel/SBA weight ratio reached 1. The N–H stretching vibration in the 3200–3500 cm^{-1} domains partially overlapped with the broad band between 3200–3600 cm^{-1} that arose from the broad absorption due to the H-bonded –OH with various OH to H distances.

After investigating the effect of the hydrogel addition on the structural and textural characteristics of mesostructured SBA-15, as a proof of concept *Mucor miehei* lipase (Mm-L) was physisorbed onto SBA-15 and the adsorption was followed by the addition of the hydrogel to reduce the mesopore diameter. In this way, we were able to partially close the mesopores after the enzyme immobilization. Indeed, in a previous paper we demonstrated that SBA-15 could be used as a matrix for physisorbed Mm-L, but the enzyme was released after the first cycle of the reaction.

3.2. Lipase immobilization on SBA-15 followed by hydrogel incorporation

As depicted in Fig. 5A(a), (b) and B(a), (b), upon Mm-L adsorption, the hexagonal structure and the type IV nitrogen adsorption–desorption isotherm of the SBA-15 support were maintained, but the adsorbed volume decreased (Fig. 5B(a) and (b)). At the same time, there was a decrease in the dV/dD value in the pore-size distribution (Fig. 5C(a) and (b)), and of the specific surface area from 710 to 235 $m^2\ g^{-1}$ and of the pore volume from 0.81 to 0.31 $cm^3\ g^{-1}$. The average mesopore diameter also decreased from 9.7 to 8.9 nm (Fig. 5C(a) and (b)). Considering the changes in the textural properties in the presence of the lipase as well as the spherical molecular diameter of Mm-L, which was around 3.0–4.0 nm,[46] we concluded that the enzyme was adsorbed in the mesopores of the SBA-15 support. Nevertheless, we could not exclude that the enzyme might not have deeply penetrated into the pores and that

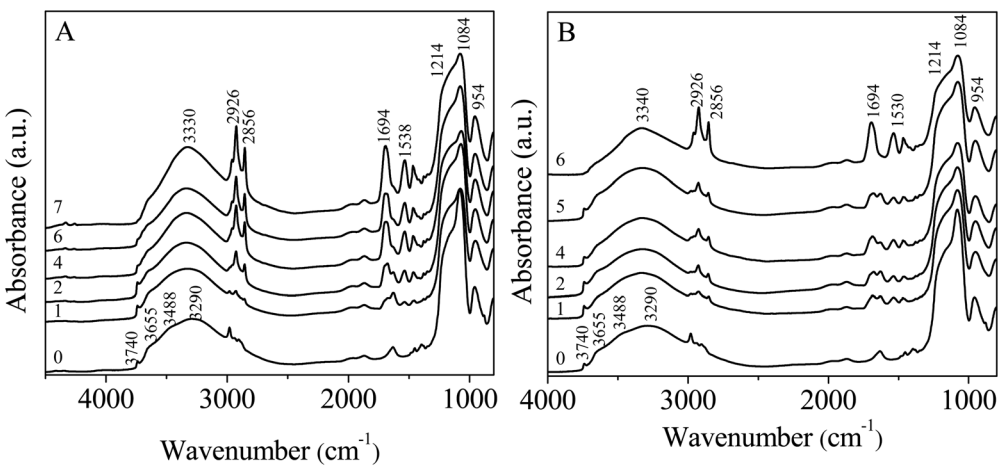

Fig. 4 Infrared spectra as a function of the hydrogel/SBA weight ratio. The hydrogel contains 5 wt% (A) or 10 wt% of tetradecylcarbamate (B).

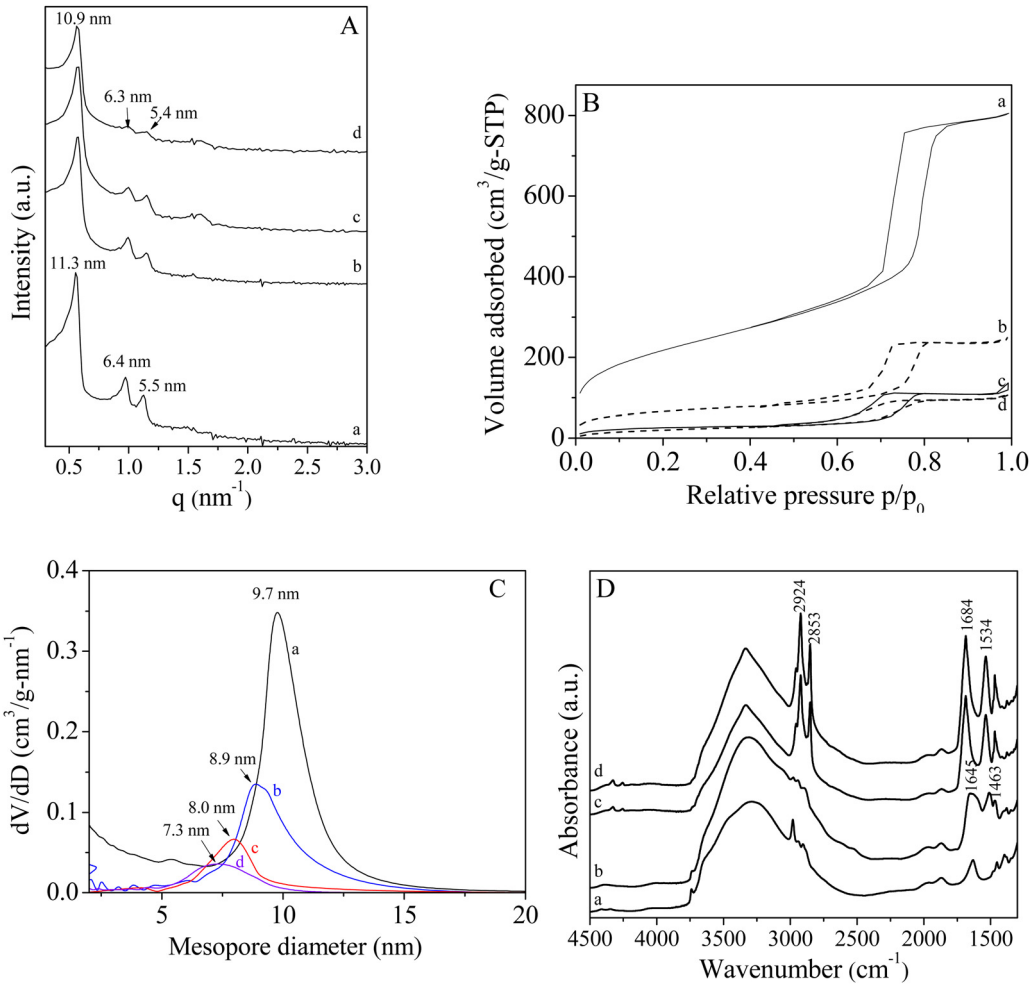

Fig. 5 Pattern (A), nitrogen adsorption–desorption isotherm (B), mesopore size distribution (C) and infrared spectrum (D) of: SBA-15 (a), SBA-15 after physisorption of Mm-L (b) and the biocatalyst after gel incorporation (c) and (d). The gel contains either 5 wt% (c) or 10 wt% (d) of tetradecylcarbamate.

the external surface was also involved in the adsorption. The presence of the enzyme on SBA-15 was evidenced by infrared spectroscopy (Fig. 5D(a) and (b)). Indeed, the major absorption bands of the peptide's group vibrations were observed in the range between 1200–2000 cm^{-1}. The amide I band (1600–1700 cm^{-1}) predominantly originated from the C=O stretching vibrations of the peptide bond groups, while the amide II band (1510–1680 cm^{-1}) arose from the N–H in-plane bending and C–N stretching modes of the polypeptide chains.

The amide III band arising from the N–H bending, C–Cα and C–N stretching vibration was detected at 1463 cm^{-1} (Fig. 5Db). Using the same methodology to the one reported in ref. 40, we determined that 0.28 mg of enzyme per mg of material was adsorbed. After the Mm-L physisorption, the hydrogel was incorporated in the material to reduce the mesopore diameter. The weight ratio between the hydrogel and SBA-15 loaded with Mm-L was fixed at 7 since this ratio induced a significant reduction of the mesopore diameter. Hydrogels prepared with 5 or 10 wt% of tetradecylcarbamate were considered. As in the absence of enzyme, the hexagonal mesostructure was maintained when the hydrogel was added. Indeed, whatever the tetradecylcarbamate content in the hydrogel, the peaks characteristic of the (100), (110) and (200) planes were clearly observed in the SAXS pattern without any significant modification of their position in comparison with the SAXS pattern of SBA-15 loaded with Mm-L (Fig. 5A and B-(d)). Referring to this material, we note also that a type IV isotherm was still obtained in the nitrogen adsorption–desorption analysis, reflecting the mesoporous features of the materials. However, a supplementary decrease in the volume of nitrogen adsorbed was observed (Fig. 5B(b)–(d)). We also noted additional drops in the values of the specific surface area and the pore volume from 235 to 91 m^2 g^{-1} or 79 m^2 g^{-1} and from 0.31 to 0.14 cm^3 g^{-1} or 0.13 cm^3 g^{-1} in the presence of the hydrogel containing 5 or 10 wt% of carbamate. More interesting, in the presence of the hydrogel prepared with 5 or 10 wt% of tetradecylcarbamate, the mesopore diameter was further reduced from 8.9 to 8.0 nm or 7.4 nm. The vibrations characteristic of the C=O and N–H groups of the gels were also detected by infrared spectrometry (Fig. 5Dc, d); however, they unfortunately overlapped the ones of the enzyme.

Afterwards, the material with the hydrogel was tested as a catalyst for the transesterification reaction. Using the same

reaction conditions as for the material without the hydrogel, the transesterification yields were 83% and 66% after the incorporation in the support of the hydrogel containing 5 and 10 wt% of carbamate, respectively. Herein, we have reported the reaction yield, which was calculated by considering the limiting reagent (methanol in our case) and not the conversion of the fatty acids, which indeed had a theoretical maximum value of 33%. Comparing these results with the yield obtained for Mm-L-SBA-15, the conversion yield with the hydrogel was slightly higher with 5 wt% of carbamate (76% for Mm-L-SBA-15, obtained in previous studies[40,41]). This could be due to a change in the accessibility of the active sites of the enzyme when incorporating the hydrogel in the biocatalyst, but this phenomenon was limited by the amount of the hydrogel incorporated in this study. Moreover, the same reaction was done but this time with a molar ratio of methanol to oil equal to 3, to see if the hydrogel would have a protective role for the enzyme against methanol toxicity. The obtained yield was equal to 4%, indicating that even in the presence of the hydrogel, the methanol could still damage the lipase as observed in our previous study[41] and additionally, the methanol probably dissolved the hydrogel surrounding the enzyme.

Next, the repeated use ability of the biocatalyst prepared in the presence of the hydrogel was evaluated and its efficiency compared to that of the biocatalyst prepared without the hydrogel.[40,41] After each run, the material containing lipase was washed with hexane and filled with fresh substrate solution for the next batch. The initial activity prior to the first recovery was taken as 100%. The relative efficiency of the biocatalyst for the transesterification with repeated use of the immobilized lipase on the mesoporous materials is shown in Fig. 6.

From this figure, it could be observed that in the presence of the hydrogel the supported biocatalyst could be used 4 times before losing 90% of its activity *vs.* only 2 consecutive runs for Mm-L-SBA-15, as reported elsewhere.[40] This demonstrates the utility of the hydrogel to partially preserve the activity of the biocatalyst and clearly suggests that the leaching of the enzyme was strongly diminished by the addition of the hydrogel, which reduced the mesopore size. However, as explained above, the methanol used for the reaction likely dissolved the gel and after each run a part of the enzyme was probably released. As a consequence, the efficiency decreased after each use. However, even though its activity decreased, it still showed better efficiency than the corresponding physisorbed enzyme on SBA-15, for up to 5 consecutive runs. The dissolution of the gel was supported by the mesopore size distribution, in which the maximum size was shifted from 6.6 to 8.1 nm after the second run (Fig. 7). This clearly indicates that a part of the gel had been removed during the transesterification reaction. From these results, it seems that the most promising applications for these materials are reactions in organic media, such as the methanolysis of rapeseed oil in hexane. This will be the subject of a further publication. In this way, we expect that the dissolution of the gel could be avoided and the reusability of the supported catalyst could be enhanced.

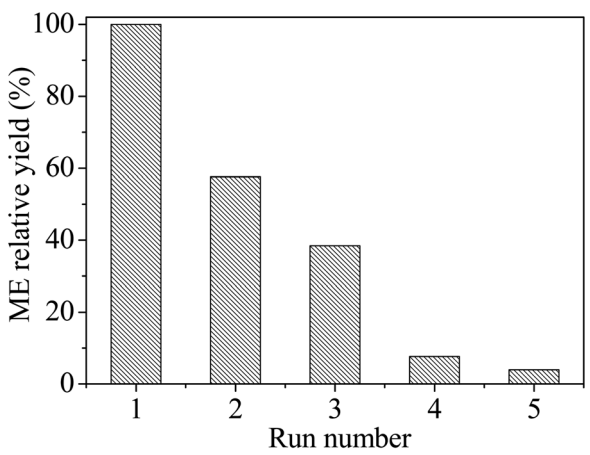

Fig. 6 Variation of methyl ester (ME) yield over the recycling runs.

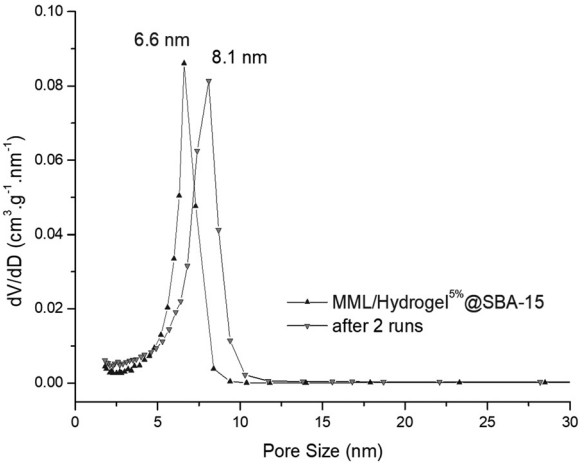

Fig. 7 Mesopore size distribution of the as-prepared supported biocatalyst (▲) and after 2 runs (▽).

4. Conclusion

In the present study, we first investigated the ability of a supramolecular biosourced hydrogelator to be used to control the pore diameter of mesostructured silica (SBA-15). The materials were characterized by SAXS, nitrogen gas adsorption and infrared spectroscopy. The infrared spectra proved the presence of the hydrogel, while the SAXS patterns and nitrogen isotherms confirmed that the mesopore ordering was preserved and that the hydrogel could be used to reduce the mesopore diameter.

Next, the immobilization of *Mucor Miehei* lipase onto the silica support, followed by the addition of the hydrogel was carried out. This supported biocatalyst effectively catalyzed the transesterification of rapeseed oil with methanol with transesterification yields of 83% and 66% after the incorporation in the support of the hydrogel containing 5 and 10 wt% of carbamate, respectively, against a yield of 76% for the biocatalyst without the hydrogel. Moreover, the biocatalyst showed higher operational stability. However, because the methanol likely dissolved a part of the hydrogel, the efficiency of the supported biocatalyst decreased after each run due to enzyme leaching.

Author contributions

Christine Gérardin: writing – original draft, supervision. Karine Assaker: investigation. Mélanie Emo: investigation, formal analysis. François Vibert: investigation. Jean-Luc Blin: writing – original draft, supervision.

Data availability

All data are included in the manuscript. If the reviewers require ESI,† they will be provided upon request by the authors.

Conflicts of interest

There are no conflicts to declare.

Acknowledgements

The authors would like to thank Sandrine Adach from the Synbion platform of L2CM for her help and fruitful discussions regarding the gas chromatography technique. LERMAB is supported by a grant overseen by the French National Research Agency (ANR), as part of the ''Investissements d'Avenir'' program (ANR-11-LABX-0002-01, Lab of Excellence ARBRE). The authors acknowledge financial support from the ''Impact Biomolecules'' project of the ''Lorraine Université d'Excellence'' (Investissements d'avenir – ANR 15-004).

References

1 P. Botella, A. Corma and M. Quesada, *J. Mater. Chem.*, 2012, **22**, 6394.
2 S. Y. Park, M. Barton and P. Pendleton, *Colloids Surf., A*, 2011, **385**, 256.
3 X. Zhang, V. Thavasi, S. G. Mhaisalkar and S. Ramakrishna, *Nanoscale*, 2012, **4**, 1707.
4 L. Braganca, M. Ojeda, J. L. G. Fierro and M. I. Pais da Silva, *Appl. Catal., A*, 2012, **423–424**, 146.
5 J. L. Blin, C. Gérardin, C. Carteret, L. Rodehüser, C. Selve and M. J. Stébé, *Chem. Mater.*, 2005, **17**, 1479.
6 P. Reis, T. Witula and K. Holmberg, *Microporous Mesoporous Mater.*, 2008, **110**, 355.
7 S. Hudson, E. Magner, J. G. Wall and B. K. Hodnett, *J. Phys. Chem. B*, 2005, **109**, 19496.
8 J. Deere, E. Magner, J. G. Wall and B. K. Hodnett, *Catal. Lett.*, 2003, **85**, 19.
9 Z. Zhou and M. Hartmann, *Chem. Soc. Rev.*, 2013, **42**, 3894.
10 M. Hartmann, *Chem. Mater.*, 2005, **17**, 4577.
11 C.-H. Lee, T.-S. Lin and C.-Y. Mou, *Nano Today*, 2009, **4**, 165.
12 M. Bila and H. M. N. Iqbal, *Coord. Chem. Rev.*, 2019, **388**, 1.
13 M. Kim, J. Kim, J. Lee, H. Jia, H. Na, J. Youn, J. Kwak, A. Dohnalkova, J. Grate, P. Wang, T. Hyeon, H. Park and H. Chang, *Biotechnol. Bioeng.*, 2007, **96**, 210.
14 A. Salis, M. F. Casula, M. S. Bhattacharyya, M. Pinna, V. Solinas and M. Monduzzi, *ChemCatChem*, 2010, **2**, 322.
15 A. R. Sheldon and S. van Pelt, *Chem. Soc. Rev.*, 2013, **42**, 6223.
16 B. Thangaraj and P. R. Solomon, *ChemBioEng Rev.*, 2019, **6**, 167.
17 E. Magner, *Chem. Soc. Rev.*, 2013, **42**, 6213.
18 H.-X. Zhou and K. A. Dill, *Biochemistry*, 2001, **40**, 11289.
19 Y. Wang and F. Caruso, *Chem. Mater.*, 2005, **17**, 953.
20 L. Bayne, R. V. Ulijn and P. J. Halling, *Chem. Soc. Rev.*, 2013, **42**, 9000.
21 J. S. Beck. *U.S. Pat.*, US057296, 1991.
22 M. F. Ottaviani, A. Moscatelli, D. Desplantier-Giscard, F. Di Renzo, P. Kooyman and A. Galarneau, *J. Phys. Chem. B*, 2004, **108**, 12123.
23 D. Zhao, J. Feng, Q. Huo, N. Melosh, G. H. Fredrickson, B. F. Chmelka and G. D. Stucky, *Science*, 1998, **279**, 548.
24 A. Sayari, Y. Yang, M. Kruk and M. Jaroniec, *J. Phys. Chem. B*, 1999, **103**, 3651.
25 M. Kruk and L. Cao, *Langmuir*, 2007, **23**, 7247.
26 J. L. Blin and B. L. Su, *Langmuir*, 2002, **18**, 5303.
27 J. L. Blin and M. J. Stébé, *Microporous Mesoporous Mater.*, 2005, **87**, 67.
28 N. Baccile, F. Babonneau, B. Thomas and T. Coradin, *J. Mater. Chem.*, 2009, **19**, 8537.
29 C. Gérardin, J. Reboul, M. Bonne and B. Lebeau, *Chem. Soc. Rev.*, 2013, **42**, 4217.
30 J. A. Martens, J. Jammaer, S. Bajpe, A. Aerts, Y. Lorgouilloux and C. E. A. Kirschhock, *Microporous Mesoporous Mater.*, 2011, **140**, 2.
31 N. M. Sangeetha and U. Maitra, *Chem. Soc. Rev.*, 2005, **34**, 821.
32 L. Minghua, O. Guanghui, N. Dian and S. Yutao, *Org. Chem. Front.*, 2018, **5**, 2885.
33 E. R. Draper and D. J. Adams, *Langmuir*, 2019, **35**, 6506.
34 N. Basu, A. Chakraborty and R. Ghosh, *Gels*, 2018, **4**, 52.
35 W. W. Fang, Y. Zhang, J. J. Wu, C. Liu, H. B. Zhu and T. Tu, *Chem. – Asian J.*, 2018, **13**(7), 712.
36 J. Xu, X. Zhu, J. Zhao, G. Ling and P. Zhang, *Adv. Colloid Interface Sci.*, 2023, **321**, 103000.
37 F. Obounou-Akong, P. Gérardin, M.-F. Thévenon and C. Gérardin-Charbonnier, *Wood Sci. Tech.*, 2015, **49**, 443.
38 F. Obounou-Akong, A. Pasc, M. Emo and C. Gérardin-Charbonnier, *New J. Chem.*, 2013, **37**(3), 559.
39 S. Ahmed, J. H. Mondal, N. Behera and D. Das, *Langmuir*, 2013, **29**, 14274.
40 J. Jacoby, A. Pasc, C. Carteret, F. Dupire, M. J. Stébé, V. Coupard and J. L. Blin, *Process Biochem.*, 2013, **48**, 831.
41 C. Carteret, J. Jacoby and J. L. Blin, *Microporous Mesoporous Mater.*, 2018, **268**, 39.
42 M. Hajar, F. Vahabzadeh and S. Shokrollahzadeh, *Sci. Iran., Trans. C*, 2010, **17**, 97.
43 E. P. Barret, L. G. Joyner and P. P. Halenda, *J. Am. Chem. Soc.*, 1951, **73**, 373.
44 M. Thommes, K. Kaneko, A. V. Neimark, J. P. Olivier, F. Rodriguez-Reinoso, J. Rouquerol and K. S. W. Sing, *Pure Appl. Chem.*, 2015, **87**, 1051.
45 A. Galarneau, H. Cambon, F. Di Renzo, R. Ryoo, M. Choi and F. Fajula, *New J. Chem.*, 2003, **27**, 73.
46 A. Galarneau, M. Mureseanu, S. Atger, G. Renard and F. Fajula, *New J. Chem.*, 2006, **30**, 562.